• Original Paper •

Organizational Modes of Severe Wind-producing Convective Systems over North China

Xinlin YANG[1,2] and Jianhua SUN[*1,2]

[1]*Key Laboratory of Cloud-Precipitation Physics and Severe Storms, Institute of Atmospheric Physics,
Chinese Academy of Sciences, Beijing* 100029*, China*
[2]*University of Chinese Academy of Sciences, Beijing* 100049*, China*

ABSTRACT

Severe weather reports and composite radar reflectivity data from 2010–14 over North China were used to analyze the distribution of severe convective wind (SCW) events and their organizational modes of radar reflectivity. The six organizational modes for SCW events (and their proportions) were cluster cells (35.4%), squall lines (18.4%), nonlinear-shaped systems (17.8%), broken lines (11.6%), individual cells (1.2%), and bow echoes (0.5%). The peak month for both squall lines and broken lines was June, whereas it was July for the other four modes. The highest numbers of SCW events were over the mountains, which were generally associated with disorganized systems of cluster cells. In contrast, SCW associated with linear systems occurred mainly over the plains, where stations recorded an average of less than one SCW event per year. Regions with a high frequency of SCW associated with nonlinear-shaped systems also experienced many SCW events associated with squall lines. Values of convective available potential energy, precipitable water, 0–3-km shear, and 0–6-km shear, were demonstrably larger over the plains than over the mountains, which had an evident effect on the organizational modes of SCW events. Therefore, topography may be an important factor in the organizational modes for SCW events over North China.

Key words: severe convective wind, organizational mode, convective system, topography

Citation: Yang, X. L., and J. H. Sun, 2018: Organizational modes of severe wind-producing convective systems over North China. *Adv. Atmos. Sci.*, **35**(5), 540–549, https://doi.org/10.1007/s00376-017-7114-2.

1. Introduction

Developments in meteorological satellites and radar have promoted the study of the organization and evolution of convective systems. Satellite data are used to classify mesoscale convective systems (MCSs) and to describe their evolution (Maddox, 1980; Jirak et al., 2003). The application of radar techniques to meteorology has led to growth in the study of MCSs and severe convective weather (Parker and Johnson, 2000; Klimowski et al., 2003; Gallus et al., 2008; Duda and Gallus, 2010; Schoen and Ashley, 2011; Smith et al., 2012, 2013).

The regulations from the Severe Weather Prediction Center of the China Meteorological Administration (CMA) define any wind gust of $\geqslant 17$ m s^{-1} as a severe wind event. In the study by Yang et al. (2017), if a severe wind event was associated with severe thunderstorms, it was classified as severe convective wind (SCW). Many convective systems can cause SCW events, such as bow echoes (Fujita, 1978; Przybylinski, 1995; Weisman, 2001; Klimowski et al., 2004),

squall lines (Bluestein and Jain, 1985; Smull and Houze, 1985; Parker and Johnson, 2000), and supercells (Moller et al., 1994). In the USA, tornadoes tend to be associated with supercells, whereas non-tornadic severe wind events are caused mainly by bow echoes, squall lines, and broken lines (Klimowski et al., 2003; Duda and Gallus, 2010; Schoen and Ashley, 2011; Smith et al., 2012, 2013). The dominating organizational modes associated with SCW may change with geography (Gallus et al., 2008; Smith et al., 2013). For instance, severe gusts caused by quasi-linear convective systems are most frequent in the plains and the Midwest regions, whereas severe gusts with disorganized storms are mainly in the plains and the Intermountain West (Smith et al., 2013).

The evolution of thunderstorms is affected by dynamic and thermodynamic conditions, and organizational modes can affect the type of weather events to some extent (Gallus et al., 2008; Duda and Gallus, 2010; Zheng et al., 2013). SCW events occur frequently over North China (Yang and Sun, 2014; Yang et al., 2017), but there have been only a few studies on these events.

In this paper, we focus on the following two questions: Which of the primary organizational modes are responsible for SCW events over North China? And do the organizational

---

* Corresponding author: Jianhua SUN
  Email: sjh@mail.iap.ac.cn

modes show a particular spatial distribution?

2. Data and methods

2.1. *Data*

The SCW events studied here were taken from severe weather reports (SWRs) during 2010–14. The SWR data, with eight three-hour files for each day, provide information on severe weather events such as thunderstorms, wind events, hail, and dust storms, including the station ID, location, time, and type of weather phenomenon. Cloud-to-ground lightning data were used to remove some severe wind events associated with weak thunderstorms by comparing the intensities of cloud-to-ground lightning between each severe wind event and the climatic background in the same month in which the severe wind reports occurred (Yang et al., 2017). In this study, we define North China as the region covering (36°–42°N, 109°–120°E), where SCW events occur frequently (Yang and Sun, 2014; Yang et al., 2017). SCW events occurred at 264 stations over North China during the five years. Of these, 238 stations (about 90%) had five annual reports, and the remainder had three to four (Fig. 1). As there are no specific data that clarify SCW events in China, the SWR data were utilized as a best alternative. However, it is important to note that the National Meteorological Center's data collection on severe weather in the SWR data do not cover a long period. Also, the SWR data did not record all the severe wind reports over Shandong Province and Inner Mongolia during 2010–14. As such, the spatial distribution of SCW events was tightly linked to the boundary line (Fig. 1).

Composite radar reflectivity data with a 0.01° spatial resolution were used to classify the organizational mode of each SCW event. The Beijing Meteorological Service supplied radar data with a 6-min time span from June 2010 to September 2010, whereas the CMA supplied radar data with a 10-min time span for the remaining period. The radar data from the Beijing Meteorological Service omitted a small part of the study region in the west, and the radar did not record data throughout the day during the non-flood seasons from October to March. These two reasons led to roughly 15% of the SCW events (181 null events) being unclassified. The percentages of unclassified SCW events in spring and autumn were larger than that in summer. The stations with null events were located mainly in the mountainous region from the northern part of Shaanxi Province to the northwestern part of Hebei Province, whereas stations in the plains were generally without null events.

2.2. *Classification of organizational modes*

There have been many studies aimed at classifying the organizational modes of convective systems or severe weather, but no consistent classification scheme has emerged as yet. Based on some previous studies of classification schemes, the organizational modes were classified into six main categories (Fig. 2): individual cells (ICs); cluster cells (CCs); broken lines (BLs); nonlinear-shaped systems (NLs); squall lines (SLs); and bow echoes (BEs). Table 1 details the classification schemes to which we primarily referred. Notably, we did not apply the method of sub-classifying linear systems according to their stratiform echo configurations (Parker and Johnson, 2000; Gallus et al., 2008; Duda and Gallus, 2010; Zheng et al., 2013).

ICs are storms with no weak radar echoes connecting the cells (Gallus et al., 2008), and tend to evolve independently.
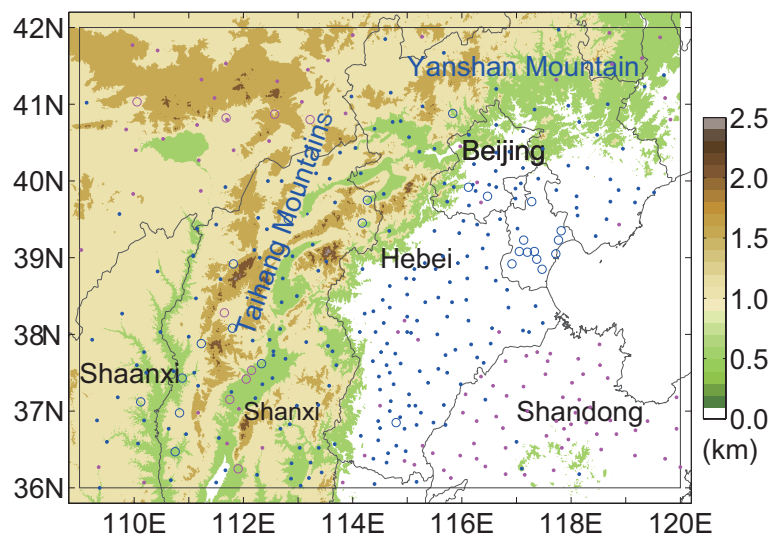

Fig. 1. Locations of stations with severe weather reports during 2010–14. Blue indicates stations that recorded severe wind events; pink indicates those stations that did not. Solid dots indicate stations with five years of records; circles indicate stations with three to four years of records. The gray box marks the region (36°–42°N, 109°–120°E). The shading indicates topography.
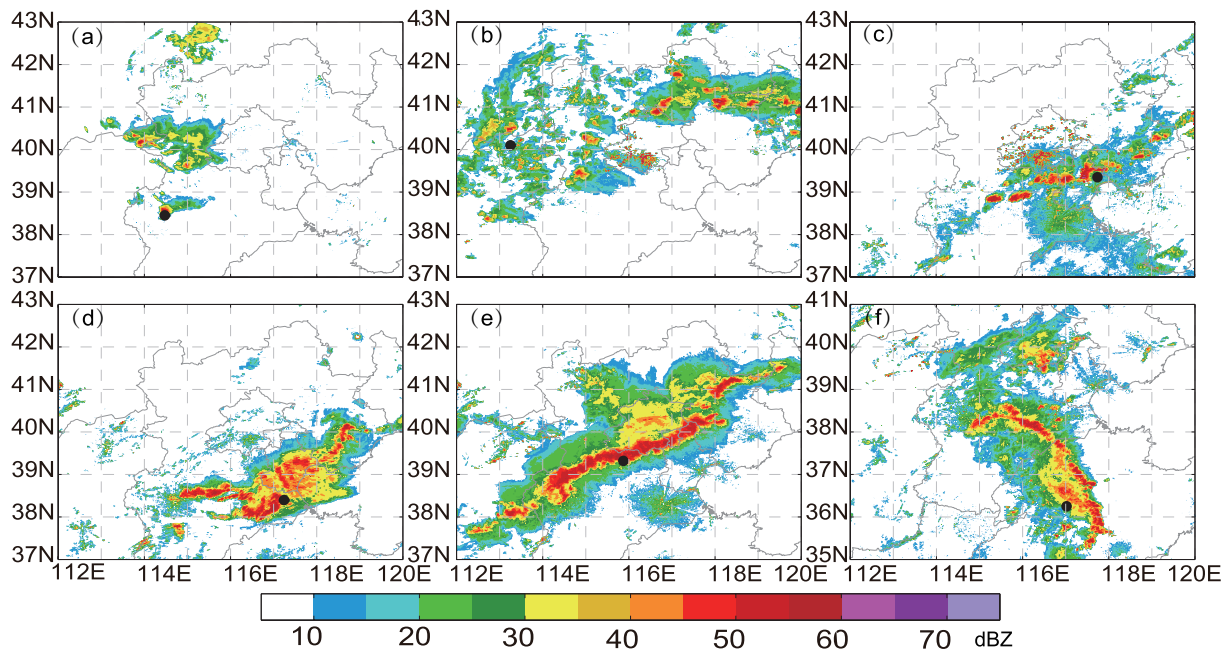
Fig. 2. Radar images of the observed (a) ICs at 1341 UTC 10 July 2010, (b) CCs at 0650 UTC 10 June 2011, (c) BLs at 1220 UTC 20 August 2012, (d) NLs at 1220 UTC 4 July 2013, (e) SLs at 1230 UTC 4 August 2013, and (f) BEs at 0340 UTC 1 August 2013. The black dot shows the location of the SCW event.

Table 1. Classification of organizational modes.

Weather events	Classification and criteria for organizational modes
Convective storms (Gallus et al., 2008; Duda and Gallus, 2010)	(a) Individual cells: no weaker radar echoes connecting the cells. (b) Clusters of cells: connected by weaker radar echoes. (c) Broken squall lines: individual cells arranged in a linear fashion. (d) Linear systems: the strongest radar echoes were organized in a connected, linear fashion at least 75 km in length and at least three times as long as wide, with these criteria present for at least 2 h. (e) Nonlinear-shaped convective systems: the strongest radar echoes were organized in a connected but nonlinear fashion.
Convective wind events that caused casualties (Schoen and Ashley, 2011)	(a) Cellular (unorganized): not fulfilling any other category; radar echoes and length without restriction; typically $\leqslant$ 90 min; cells with greatest reflectivity $\geqslant$ 5 km. (b) Cellular (quasi organized): radar echoes $\geqslant$ 40 dBZ; duration $\geqslant$ 30 min without restriction; includes individual, cluster or linear cells similar to ICs, CCs, and BLs, respectively. (c) Cellular (organized): supercell or supercell embedded in an organized linear system. Supercell meets the following two criteria: (1) one or more reflectivity features indicative of the presence of a supercell (e.g., radar echoes $\geqslant$ 40 dBZ; inflow notch, hook echo, tight reflectivity gradient, V-shaped notch, or storm splits); (2) a persistent (at least six radar scans or 30 min) mesocyclone as identified and confirmed by multiple elevation slices of storm-related velocity data. (d) Linear (organized): radar echoes $\geqslant$ 40 dBZ connected by weaker radar echoes arranged in a linear or quasi-linear fashion or a line-echo wave pattern; duration $\geqslant$ 30 min, length $\geqslant$ 75 km.

Because ICs tend to develop during the nascent or declining stage, they are generally short-lived. CCs are storm cells connected by radar echoes of no more than 10 dBZ and are not distributed linearly. BLs are storm cells that are linearly distributed and have echoes of at least 35 dBZ without being connected.

Linear systems are associated with radar echoes of at least 35 dBZ being contiguous over an area of at least 900 km^2, are organized in a linear fashion of at least 75 km in length, and are at least three times as long as they are wide (Gallus et al., 2008; Duda and Gallus, 2010; Zheng et al., 2013), with these criteria being present for at least 30 min (Klimowski et al., 2003; Schoen and Ashley, 2011). The linear systems were subdivided into SLs and BEs. BEs were defined using

the method of Schoen and Ashley (2011), which is consistent with those of Fujita (1978) and Klimowski et al. (2003). BEs were defined as a bow- or crescent-shaped radar echo that had a tight reflectivity gradient on its convex (i.e., leading) edge. These storms were required to have either a persistent arc or a radius that increased with time. If a linear system did not meet the criteria of a BE, it was deemed an SL. In contrast to linear systems, NLs were those with radar echoes of at least 35 dBZ connected over an area of at least 900 km², but that did not satisfy all the other criteria.

The identification processes are summarized in the flowchart shown in Fig. 3. Firstly, the closest mosaic data prior to the SCW event were used to ascertain which storm cells caused the SCW event, although sometimes it was difficult to do. In such situations, the SCW event was assumed to have been caused by convection over a $2° \times 2°$ region centered on the location of the SCW. Then, the organizational mode of the candidate morphology was identified for each SCW event. If the distribution of storm cells seemed likely to be an SL or a BE, continuity had to be checked in the temporal dimension.

Supercells are highly related to severe gusts in the USA (Klimowski et al., 2003; Duda and Gallus, 2010; Schoen and Ashley, 2011; Smith et al., 2012). However, we did not consider supercells in the present study for the following reasons: Firstly, according to local forecasters, supercells rarely occur over North China. In addition, during the process of classification, only a few SCW events had radar features typical of a supercell, such as a hook echo, a rear inflow notch, or storm splits. Finally, previous studies used mesocyclone data from the Principal User Processor to identify supercells (Yu et al., 2006), but such data are not saved routinely by the CMA.

The organizational modes were classified over wide spatial and temporal ranges, from ICs on small spatial and temporal scales to linear systems that persisted for several hours and extended over hundreds of kilometers. However, it was difficult to accurately classify the organizational mode of every SCW event—a difficulty experienced in many other related studies (Klimowski et al., 2003; Gallus et al., 2008; Duda and Gallus, 2010; Schoen and Ashley, 2011; Smith et al., 2012, 2013). The organizational mode changed at different stages of the convective system. Sometimes, the candidate mosaic was in the state when one mode was evolving into another; for instance, an SCW event occurred in the process of changing from an SL to a BE. In addition, it was difficult to identify the organizational modes if the candidate mosaic did not fit well with the morphology of a specific mode; for instance, a potential mosaic may have met the appearance of a specific mode, but the intensity of the radar echo was slightly weaker than that required.

2.3. *Creating proximity soundings*

The results described later, in section 3, show that CCs were the predominant organizational mode for SCW over the mountains, whereas it was SLs over the plains. To establish why this was so, we compared certain environmental parameters between the mountains and the plains. Proximity soundings were used to compute certain moisture, kinematic, and thermodynamic variables. The spatial and temporal resolutions of the sounding observations were too coarse to represent the environment of an SCW event, so instead we used the higher-resolution global final-analysis data from the National Centers for Environmental Prediction (NCEP FNL) to create proximity soundings (Lee, 2002; Brooks et al., 2003). However, this approach cannot reproduce low-altitude or surface-based parameters (Lee, 2002). Therefore, following Johnson and Bresch (1991), we used automatic surface observation data to correct the low layers of the proximity soundings to compensate for the strong vertical gradients associated with the lower atmosphere.

The steps taken to create and correct the soundings were as follows: Firstly, we collected a total of 20 layers (200–1000 hPa) of information on temperature, moisture, wind, and height at the grid nearest the SCW event from the NCEP FNL data before the SCW event occurred. Then, we removed those layers whose heights were less than the altitude of the surface station reporting the SCW event. Next, we interpolated the temperature, dew-point temperature, and pressure at
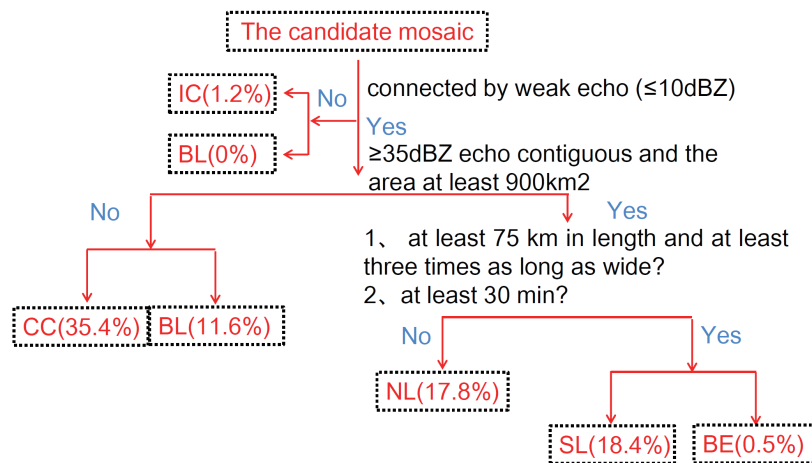

Fig. 3. Flowchart for identifying organizational modes.

the surface station at which the SCW event occurred to one hour earlier than the event by using automatic surface observation data with a 1-h resolution. If the interpolated surface temperature rising along the dry adiabatic line crossed with the temperature profile of the previous sounding from NCEP FNL, the temperature profile below the crossing layer was replaced by the dry adiabatic line rising from the interpolated surface temperature. If they did not cross, the interpolated surface data were deemed the lowest layer of the proximity sounding. Thermodynamic variables were computed from the last proximity sounding, while the 0–3-km vertical shear (SHR3) and 0–6-km vertical shear (SHR6) were the magnitude of the vector difference between the surface and 3 km or 6 km, respectively, above the ground-level winds.

3. Results

3.1. *Distribution of SCW events over northern China*

In 2010–14, SCW occurred frequently over North China around midafternoon from March–October, with 80.1% of events occurring during the summer (June–August). In the five years studied, there were 1198 SCW events over 226 days, 62.8% of which (142 days) involved fewer than three SCW events per day (Fig. 4a). The largest number of SCW events to occur on a single day was 74. The highest frequency of SCW was located over the mountainous region from the

northern part of Shaanxi Province to the northwestern part of Hebei Province: on average, a station located there recorded more than one SCW per year (Fig. 4b). Averages of less than one SCW per year were located mainly over the plains, over the region from the east of Shaanxi Province to the west of Shanxi Province, and over the valleys of the Taihang Mountains. Hence, topography appears to be an important factor in the spatial distribution of SCW events over North China.

3.2. *Characteristics of SCW event organizational modes*

The organizational mode of each SCW was identified using the flowchart shown in Fig. 3. The proportions of the six organizational modes were as follows: 35.4% (CCs); 18.4% (SLs); 17.8% (NLs); 11.6% (BLs); 1.2% (ICs); and 0.5% (BEs) (Fig. 3). The majority of SCW events were assigned to the CC class. These results show that the SCW events were caused mainly by weak organized and nonlinear-shaped convective systems, and that linear convective systems (SLs and BEs) accounted for 18.9% of the SCW events. In North America, severe gusts are caused mainly by organized systems (Klimowski et al., 2003; Smith et al., 2012, 2013). This shows that the major organizational modes of SCW events change according to region.

In general, SCW events occurring in April–August were frequently those with CC modes (Fig. 5). The peak months were June or July for the six modes (Fig. 5). For instance, June was the peak month for linear and organized systems
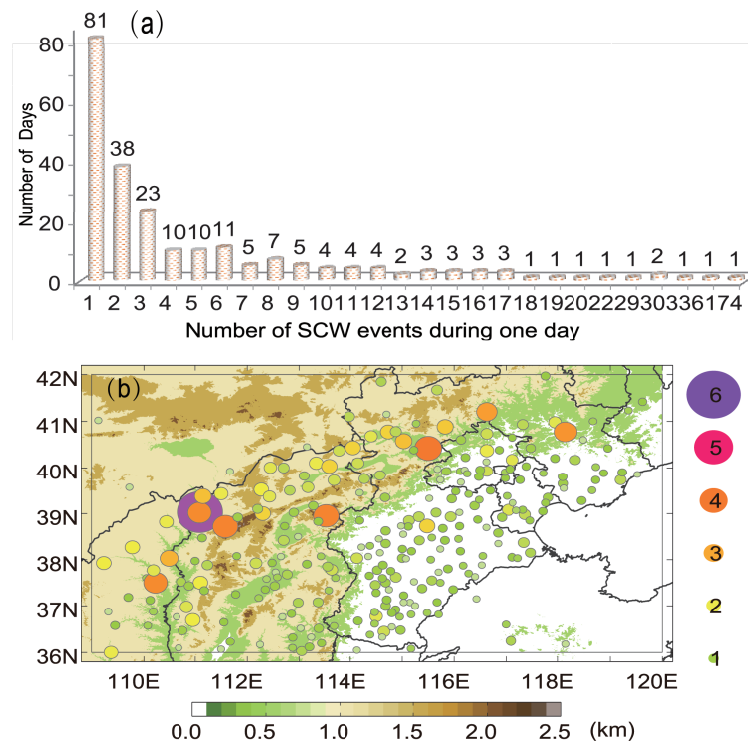

Fig. 4. (a) Frequency of days with various numbers of severe wind events occurring over North China. (b) Spatial distribution of annual mean number of SCW events. The dots are sized according to the number of severe wind events. The shading indicates topography. The box marks the region (36°–42°N, 109°–120°E).

(SLs and BLs), whereas the peak month for nonlinear-shaped systems (CCs and NLs) was July.

ICs tend to operate on small spatial and temporal scales, so SCW events with ICs are usually caused by local storms. In 2010–14, 14 stations recorded a total of 14 IC events over North China; these occurred in May–September, with six IC events in July (Fig. 5). Overall, the proportion of IC events was very low each month. The spatial distribution of IC events was decentralized, with many located over regions of low elevation (not shown). IC events accounted for less than 20% of all SCW events for most stations reporting an IC event.

The majority of SCW events (35.4%) were CC classes, most of which occurred in May–August. The number of CC events increased rapidly in June, leading to July being the peak month with 148 (Fig. 5). The largest number of CC events occurring at a single station reached 17 during 2010–14, whereas fewer than seven occurred at most stations (Fig. 6a). The regions with the highest frequency of CC events were from the north of Shanxi Province to the northwest of Hebei Province (Fig. 6a), while there were clearly fewer over the region from central Shanxi Province to the south of Hebei Province. CC events over those two regions accounted for 40%–70% of all SCW events (Fig. 6b). In North America, IC and CC events are also more frequent over the western part of the Midwest, which lies at a higher elevation than the eastern part (Gallus et al., 2008).

BL events accounted for only a small proportion of all SCW events and occurred mainly during both June (56.8%) and July (16.5%) (Fig. 5). Of all the SCW events that occurred in June, 19.3% were associated with BLs. BL events occurred frequently over the region from the northern part of Shaanxi Province to the northwestern part of Shanxi Province, where 10%–40% of SCW events were BL classes (Fig. 7). Two other regions over which many stations recorded BL events were the transition zones between mountains and plains—from the mid-eastern part of Shanxi Province to the southern part of Hebei Province, and the southern part of the Yanshan Mountain. However, most stations in those two regions recorded only one BL event during the five years.

NLs occurred mainly in May–August. 22.7% of SCW events in July were NLs (Fig. 5). NL events occurred frequently over three regions: the eastern part of the plains; the area from the mid-eastern part of Shaanxi Province to the mid-western part of Shanxi Province; and the northeastern part of Shanxi Province (Fig. 8a). NL events accounted for 30%–60% over the first two regions, whereas the proportion was slightly smaller over the third region (Fig. 8b).

SL events also occurred mainly during the summer, with 42.1% in June (Fig. 5). SL and BL events had the same peak month because the latter generally developed into linear
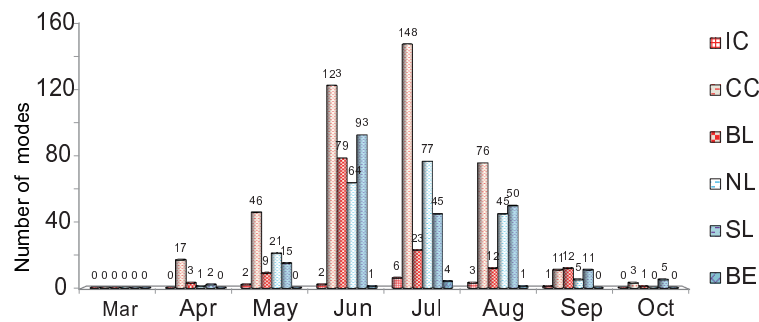

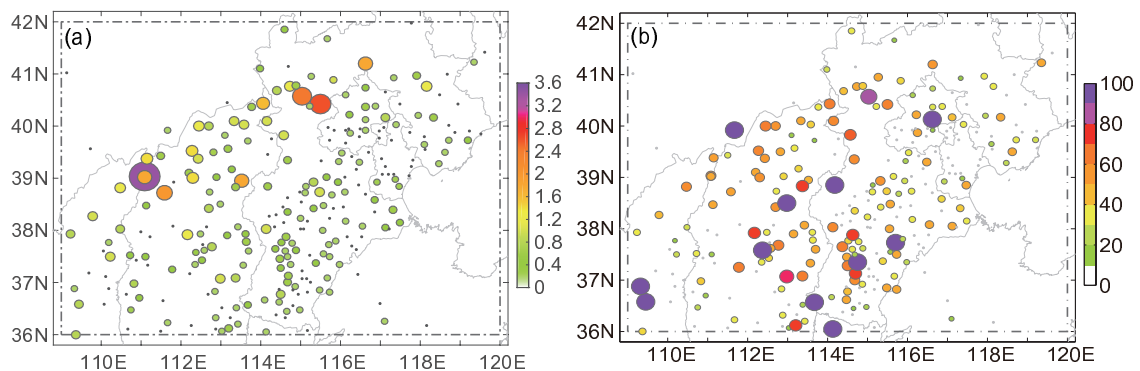Fig. 5. Monthly distributions of various organizational modes.

Fig. 6. Spatial distribution of (a) the annual mean number of CC-type severe wind events and (b) the proportion of CC-type severe wind events to all severe wind events. Gray dots show stations at which only non-CC severe wind occurred. The box marks the region (36°–42°N, 109°–120°E).
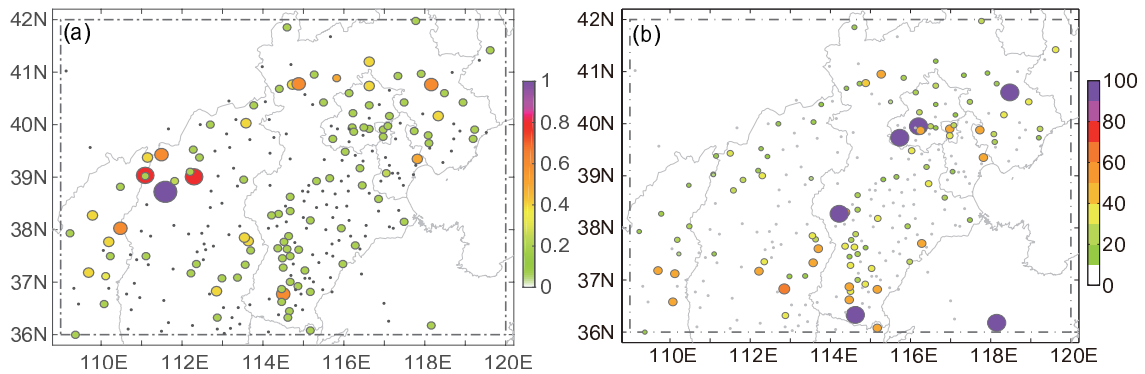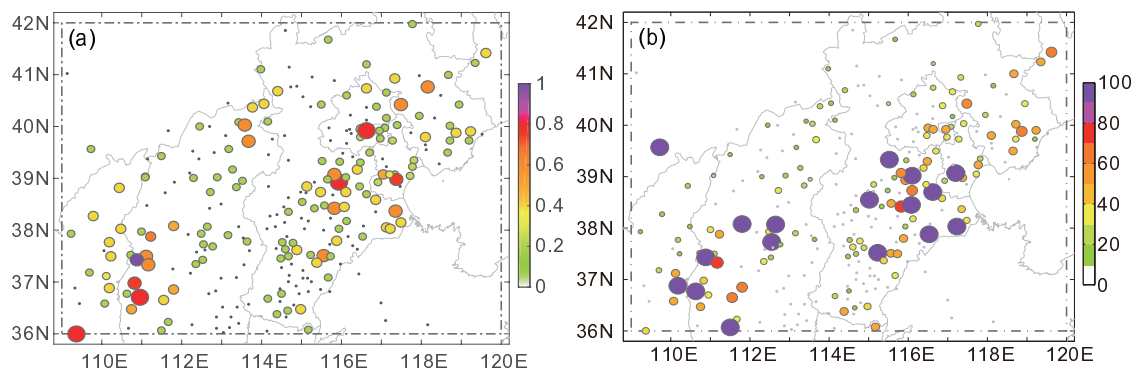
Fig. 7. As in Fig. 6 but for BLs.

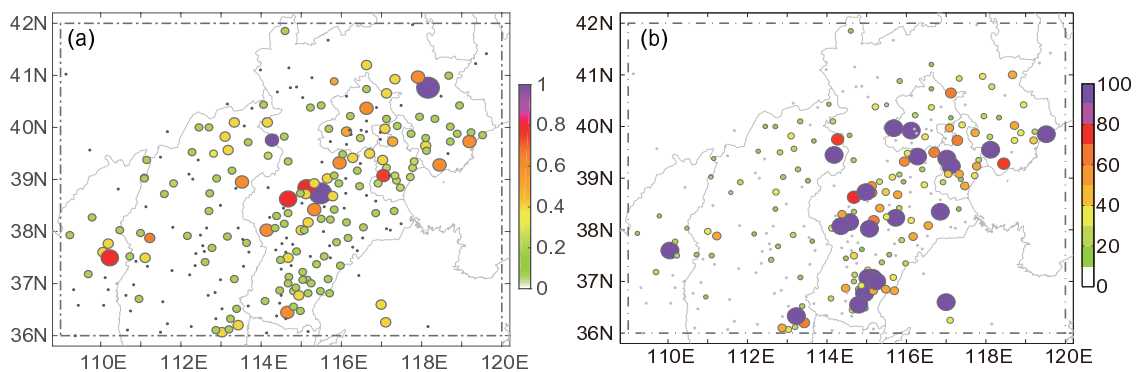**Fig. 8.** As in Fig. 6 but for NLs.

Fig. 9. As in Fig. 6 but for SLs.

convective systems. Supercell and linear convective systems occur frequently in June in North America, whereas disorganized systems (CCs and ICs) are associated with a peak month in July (Smith et al., 2013). The peak month of organized systems of SCW over North China is consistent with that in North America. Most stations located over the plains recorded SL events (Fig. 9a). Stations that recorded more than two SL events were located over the plains, northern Shanxi Province, and the area from the mid-eastern part of Shaanxi Province to the mid-western part of Shanxi Province (Fig. 9a). The proportion of SL events was 20%–60% at stations across the plains, whereas it was less than 30% in the other two regions (Fig. 9b). Regions with high rates of SL

events also tended to have high rates of NL events (Fig. 9a and Fig. 8a).

Compared with the other types of event, there were very few BE events in the provinces of Hebei and Shandong. For instance, only six BE events were recorded among five stations during 2010–14, which is why no further details on BE events are discussed. Linear systems (SLs and BEs) occurred mainly over the plains east of the Taihang Mountains. Zheng et al. (2013) came to a similar conclusion about linear systems occurring mainly over the plains in the Jianghuai region, because thunderstorms that were triggered in the mountains spread eastward and evolved into linear systems.
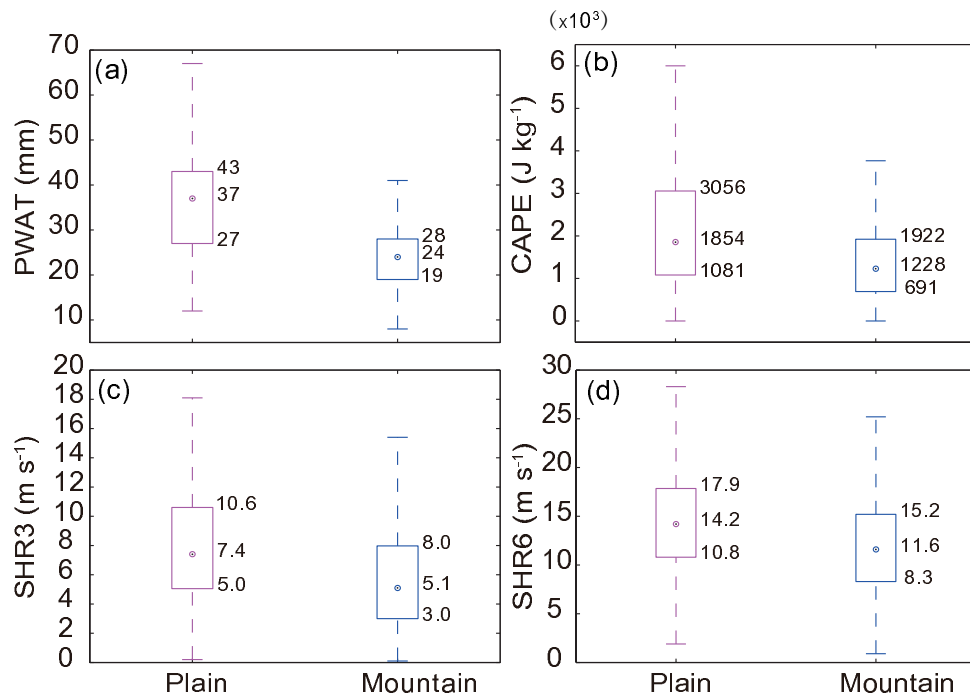
Fig. 10. (a) Box and whiskers graph of PWAT for mountains and plains. Boxes denote the 25th (Q1) to 75th (Q3) percentiles, with a dot at the median value. The whiskers extend to the extremum of $Q1 - 1.5$ $(Q3 - Q1)$ and $Q3 + 1.5 (Q3 - Q1)$. (b–d) As in (a) but for CAPE, SHR3, and SHR6, respectively.

4. Conclusions and discussion

4.1. *Conclusions*

The severe weather reports and composite radar reflectivity data from 2010–14 over North China were employed to analyze the distributions of SCW events and their organizational modes. Over the five years of data, 1198 SCW events occurred among 264 stations over a total of 226 days. There was a greater tendency for SCW to occur over the high-altitude region from the north of Shaanxi Province to the northwest of Hebei Province, while stations on the lower-lying plains recorded an annual average of less than one SCW. This implied that terrain is a major factor favoring the occurrence of SCW.

The proportions of the six organizational modes of SCW over Northern China were 35.4% (CCs), 18.4% (SLs), 17.8% (NLs), 11.6% (BLs), 1.2% (ICs), and 0.5% (BEs), among which CC events were the most common. The peak month for SLs and BLs was June, whereas it was July for the other four modes. CC-type SCW events occurred mainly over the region from the north of Shanxi Province to the northwest of Hebei Province, and over the region from the mid-eastern part of Shanxi Province to the southern part of Hebei Province; over those regions, SCW events with CC classes accounted for 40%–70% of all SCW. SCW with SL classes occurred frequently over the plains of North China, over the northeast of Shanxi Province, and over the area from the mid-eastern part of Shaanxi Province to the western part of Shanxi Province. The proportion of SL events to all SCW over the plains was 20%–60%, whereas the percentages were less than 30% over the other two regions. Regions with a high rate of NL events also had a high rate of SL events. The highest frequency of BL events occurred mainly over the region from the northern part of Shaanxi Province to the northwestern part of Shanxi Province, and BL events frequently occurred over the area between the mountains and the plains.

4.2. *Environmental differences between mountains and plains*

SCW events associated with SL classes occurred frequently over the plains, whereas CC events occurred mainly over the mountains. In North America, linear systems and supercells occur mainly to the east of the Rocky Mountains (Klimowski et al., 2003), whereas disorganized cells (ICs and CCs) occur frequently at high mountainous elevations (Gallus et al., 2008). Because the development and evolution of MCSs are controlled by the environment at the synoptic scale, the severe long-lasting thunderstorms that accompany organized systems tend to be associated with strong vertical shears (Doswell III, 1987; Brooks, 2006; Brooks et al., 2007; Wang et al., 2013). In addition, moisture and its vertical distribution are important to the intensity and morphology of convective systems (Wang et al., 2013; Sun et al., 2014).

Therefore, we used four physical variables—convective available potential energy (CAPE), precipitable water (PWAT), SHR3, and SHR6—to study the differences between the mountains and plains over North China due to synoptic-scale environmental conditions. Also, we were interested in why the organizational modes of SCW events showed a marked difference between mountains and plains. The sta-

tions with SCW events were classified into two classes according to whether their altitudes were higher (mountains) or lower (plains) than 500 m. There were 114 stations with 692 SCW events over the mountains, and 150 stations with 506 cases over the plains.

The four physical parameters were calculated for the mountains and the plains from the proximity soundings. This showed the CAPE and PWAT values for the mountains to be less than those for the plains (Fig. 10a). For instance, for 75% of the SCW events over the mountains, the PWAT value was less than 28 mm, whereas it was greater than 27 mm for about 75% of the SCW events over the plains. The median values of CAPE for the mountains and plains were 1228 J kg^{-1} and 1854 J kg^{-1}, respectively (Fig. 10b). The PWAT and CAPE values could reflect the intensity of the potential convection to some extent. The distributions of CAPE and PWAT were consistent with the conclusion that the convection of SCW over mountains tends to be weaker than that over plains.

The distributions of SHR3 and SHR6 (Figs. 10c and d, respectively) showed that the vertical shears over the mountains (especially SHR3) were also less than those over the plains. In conclusion, thunderstorms over the mountains were less intense than those over the plains, because of the dynamic and thermodynamic conditions of SCW events. Over the mountains, SCW events were generally associated with disorganized systems such as CC events, whereas the SCW events over low-lying ground were frequently associated with linear organized systems. Furthermore, there is no doubt that the development and evolution of thunderstorms are affected by the underlying topography. On the one hand, it is difficult for convection over mountains to evolve into a linear system because of friction and the blocking effect of the mountains. On the other hand, because of their far more homogeneous topography, the development and movement of convection over plains are affected mainly by atmospheric conditions. Therefore, the spatial distribution of the organizational modes of SCW over North China is due to topography and synoptic-scale environments.

In conclusion, the fact that SCW occurred at the highest rate over the mountains was generally associated with disorganized CC events, whereas SCW associated with linear systems occurred mainly over the plains. The values of PWAT, CAPE, SHR3, and SHR6 over the plains were clearly larger than those over the mountains, which affected the distribution of the organizational modes of SCW significantly. Based on our analyses of the organizational modes and physical variables of SCW, the results indicated that topography is an important factor in determining the organizational modes of SCW events over North China.

REFERENCES

Bluestein, H. B., and M. H. Jain, 1985: Formation of mesoscale lines of precipitation: Severe squall lines in Oklahoma during the spring. *J. Atmos. Sci.*, **42**(16), 1711–1732, https://doi.org/10.1175/1520-0469(1985)042<1711:FOMLOP>2.0.CO;2.

Brooks, H. E., 2006: A global view of severe thunderstorms: Estimating the current distribution and possible future changes. Preprints, *Symposium on the Challenges of Severe Convective Storms*, Atlanta, GA, American Meteorological Society, Conference CD.

Brooks, H. E., J. W. Lee, and J. P. Craven, 2003: The spatial distribution of severe thunderstorm and tornado environments from global reanalysis data. *Atmospheric Research*, **67–68**, 73–94, https://doi.org/10.1016/S0169-8095(03)00045-0.

Brooks, H. E., A. R. Anderson, K. Riemann, I. Ebbers, and H. Flachs, 2007: Climatological aspects of convective parameters from the NCAR/NCEP reanalysis. *Atmospheric Research*, **83**(2–4), 294–305, https://doi.org/10.1016/j.atmosres.2005.08.005.

Doswell III, C. A., 1987: The distinction between large-scale and mesoscale contribution to severe convection: A case study example. *Wea. Forecasting*, **2**(1), 3–16, https://doi.org/10.1175/1520-0434(1987)002<0003:TDBLSA>2.0.CO;2.

Duda, J. D., and W. A. Gallus Jr., 2010: Spring and summer midwestern severe weather reports in supercells compared to other morphologies. *Wea. Forecasting*, **25**(1), 190–206, https://doi.org/10.1175/2009WAF2222338.1.

Fujita, T. T., 1978: Manual of downburst identification for Project Nimrod. Satellite and Mesometeorology Research Paper No. 156, Department of Geophysical Sciences, University of Chicago, 104 pp.

Gallus Jr, W. A., N. A., Snook, and E. V., Johnson, 2008: Spring and summer severe weather reports over the Midwest as a function of convective mode: A preliminary study. *Wea. Forecasting*, **23**(1), 101–113, https://doi.org/10.1175/2007WAF2006120.1.

Jirak, I. L., W. R. Cotton, and R. L. McAnelly, 2003: Satellite and radar survey of mesoscale convective system development. *Mon. Wea. Rev.*, **131**(10), 2428–2449, https://doi.org/10.1175/1520-0493(2003)131<2428:SARSOM>2.0.CO;2.

Johnson, R. H., and J. F. Bresch, 1991: Diagnosed characteristics of precipitation systems over Taiwan during the May June 1987 TAMEX. *Mon. Wea. Rev.*, **119**(11), 2540–2557, https://doi.org/10.1175/1520-0493(1991)119<2540:DCOPSO>2.0.CO;2.

Klimowski, B. A., M. J., Bunkers, M. R., Hjelmfelt, and J. N., Covert, 2003: Severe convective windstorms over the northern high plains of the United States. *Wea. Forecasting*, **18**(3), 502–519, https://doi.org/10.1175/1520-0434(2003)18<502:SCWOTN>2.0.CO;2.

Klimowski, B. A., M. R., Hjelmfelt, and M. J. Bunkers, 2004: Radar observations of the early evolution of bow echoes. *Wea. Forecasting*, **19**(4), 727–734, https://doi.org/10.1175/1520-0434(2004)019<0727:ROOTEE>2.0.CO;2.

Lee, J. W., 2002: Tornado proximity soundings from the NCEP/NCAR reanalysis data. M.S. thesis, University of Oklahoma, 61 pp.

Maddox, R. A., 1980: Mesoscale convective complexes. *Bull. Amer. Meteor. Soc.*, **61**(11), 1374–1387.

Moller, A. R., C. A. Doswell III, M. P. Foster, and G. R. Woodall, 1994: The operational recognition of supercell thunder-

storm environments and storm structures. *Wea. Forecasting*, **9**(3), 327–347, https://doi.org/10.1175/1520-0434(1994)009<0327:TOROST>2.0.CO;2.

Parker, M. D., and R. H., Johnson, 2000: Organizational modes of midlatitude mesoscale convective systems. *Mon. Wea. Rev.*, **128**(10), 3413–3436, https://doi.org/10.1175/1520-0493(2001)129<3413:OMOMMC>2.0.CO;2.

Przybylinski, R. W., 1995: The bow echo: Observations, numerical simulations, and severe weather detection methods. *Wea. Forecasting*, **10**(2), 203–218, https://doi.org/10.1175/1520-0434(1995)010<0203:TBEONS>2.0.CO;2.

Schoen, J. M., and W. S., Ashley, 2011: A climatology of fatal convective wind events by storm type. *Wea. Forecasting*, **26**(1), 109–121, https://doi.org/10.1175/2010WAF2222428.1.

Smith, B. T., R. L. Thompson, J. S. Grams, C. Broyles, and H. E. Brooks, 2012: Convective modes for significant severe thunderstorms in the contiguous United States. Part I: Storm classification and climatology. *Wea. Forecasting*, **27**(5), 1114–1135, https://doi.org/10.1175/WAF-D-11-00115.1.

Smith, B. T., T. E. Castellanos, A. C. Winters, C. M. Mead, A. R. Dean, and R. L. Thompson, 2013: Measured severe convective wind climatology and associated convective modes of thunderstorms in the contiguous United States, 2003–09. *Wea. Forecasting*, **28**(1), 229–236, https://doi.org/10.1175/WAF-D-12-00096.1.

Smull, B. F., and R. A. Houze Jr, 1985: A midlatitude squall line with a trailing region of stratiform rain: Radar and satellite observations. *Mon. Wea. Rev.*, **113**(1), 117–133, https://doi.org/10.1175/1520-0493(1985)113<0117:AMSLWA>2.0.CO;2.

Sun, J. H., L. L. Zheng, and S. X. Zhao, 2014: Impact of moisture on the organizational mode and intensity of squall lines determined through numerical experiments. *Chinese Journal of Atmospheric Sciences*, **38**(4), 742–755, https://doi.org/10.3878/j.issn.1006-9895.2013.13187. (in Chinese)

Wang, X. M., X. G. Zhou, and X. D. Yu, 2013: Comparative study of environmental characteristics of a windstorm and their impacts on storm structures. *Acta Meteorologica Sinica*, **71**(5), 839–852, https://doi.org/10.11676/qxxb2013.073. (in Chinese)

Weisman, M. L., 2001: Bow echoes: A tribute to T. T. Fujita. *Bull. Amer. Meteor. Soc.*, **82**, 97–116, https://doi.org/10.1175/1520-0477(2001)082<0097:BEATTT>2.3.CO;2.

Yang, X.-L., and J.-H. Sun, 2014: The characteristics of cloud-to-ground lightning activity with severe thunderstorm wind in South and North China. *Atmospheric and Oceanic Science Letters*, **7**, 571–576, https://doi.org/10.3878/AOSL20140046.

Yang, X. L., J. H. Sun, and Y. G. Zheng, 2017: A 5-yr climatology of severe convective wind events over China. *Wea. Forecasting*, **32**(4), 1289–1299, https://doi.org/10.1175/WAF-D-16-0101.1.

Yu, X. D., X. P. Yao, T. N. Xiong, X. G. Zhou, H. Wu, B. S. Deng, and Q. Song, 2006: *Principle and Operation Application of Doppler Weather Radar*. China Meteorological Press, Beijing, 314 pp. (in Chinese)

Zheng, L. L., J. H. Sun, X. L. Zhang, and C. H. Liu., 2013: Organizational modes of mesoscale convective systems over central East China. *Wea. Forecasting*, **28**(5), 1081–1098, https://doi.org/10.1175/WAF-D-12-00088.1.